5-8-2007

Modeling of Thermodynamic Properties and Phase Equilibria for the Cu-Mg Binary System

Shihuai Zhou
Iowa State University, szhou@ameslab.gov

Yi Wang
Pennsylvania State University

Frank G. Shi
University of California - Irvine

Ferdinand Sommer
Max-Planck-Institute

Long-Qing Chen
Pennsylvania State University

See next page for additional authors

Modeling of Thermodynamic Properties and Phase Equilibria for the Cu-Mg Binary System

Abstract

The phase equilibria associated with the binary Cu-Mg system are analyzed by applying results from first-principles calculations to a general solution thermodynamics treatment. Differing from previously reported models, we employ a four-species association model for the liquid, while the terminal and intermediate solid phases are modeled as substitutional solutions with one or two sublattices, respectively. The zero-Kelvin enthalpies of formation for the intermediate compounds, Cu_2Mg-C15 (*cF24*) and $CuMg_2$-C_b (*oF48*) are computed using the Vienna Ab-initio Simulation Package (VASP). The Gibbs free energy functions for the individual phases are evaluated, and the resulting binary phase diagram is presented over the full composition range. While the phase diagram we propose exhibits only modest deviation from previously reported models of phase equilibria, our treatment provides better agreement with experimental reports of heat capacity and enthalpy of mixing, indicating a more self-consistent thermodynamic description of this binary system.

Disciplines

Metallurgy

Comments

This article is from *Journal of Phase Equilibria and Diffusion* 28 (2007): 158, doi:10.1007/s11669-007-9022-0. Posted with permission.

Authors

Shihuai Zhou, Yi Wang, Frank G. Shi, Ferdinand Sommer, Long-Qing Chen, Zi-Kui Li, and Ralph E. Napolitano

Modeling of Thermodynamic Properties and Phase Equilibria for the Cu-Mg Binary System

Shihuai Zhou, Yi Wang, Frank G. Shi, Ferdinand Sommer, Long-Qing Chen, Zi-Kui Liu and Ralph E. Napolitano

(Submitted November 2, 2006)

The phase equilibria associated with the binary Cu-Mg system are analyzed by applying results from first-principles calculations to a general solution thermodynamics treatment. Differing from previously reported models, we employ a four-species association model for the liquid, while the terminal and intermediate solid phases are modeled as substitutional solutions with one or two sublattices, respectively. The zero-Kelvin enthalpies of formation for the intermediate compounds, Cu_2Mg-C15 (*cF24*) and $CuMg_2$-C_b (*oF48*) are computed using the Vienna Ab-initio Simulation Package (VASP). The Gibbs free energy functions for the individual phases are evaluated, and the resulting binary phase diagram is presented over the full composition range. While the phase diagram we propose exhibits only modest deviation from previously reported models of phase equilibria, our treatment provides better agreement with experimental reports of heat capacity and enthalpy of mixing, indicating a more self-consistent thermodynamic description of this binary system.

1. Introduction

Given the promising mechanical, chemical, and magnetic properties of various metallic glasses and the potential widespread use of the so-called "bulk metallic glasses",[1-4] much recent attention has been given to the development of our general understanding of the thermodynamics and kinetics for glass formation and glass forming ability.[5] While alloys exhibiting promising glass formation tendency are frequently ternary, quaternary, or higher order systems,[1-4] several binary glass-forming metallic alloys have been identified. Of these, the Al-based alloys have been investigated most thoroughly.[6] In addition, glass formation has been identified in several other binary systems,[7-12] most notably including Cu-Mg,[7] Pd-Si,[8,9] and Cu-Zr.[8] By virtue of their simplicity compared with their many-component counterparts, these binary alloys present us with an opportunity to investigate the detailed relationship between the thermodynamic descriptions of relevant phase

equilibria and observed glass-forming behavior. It is in this vein that the present thermodynamic analysis of the Cu-Mg binary system is motivated. In a subsequent paper, we will model the thermodynamic properties of the undercooled liquid and examine more closely the implications regarding glass formation tendency, with respect to the competing crystalline phases.

Thermodynamic models for the binary Cu-Mg system have been offered by Coughanowr et al.[13] and by Zou and Chang.[14] While these treatments are well posed and have resulted in phase diagrams that agree well with experimental reports, there are three specific features of the modeling approaches that limit their potential applicability to more general phase stability problems. First, in each of these treatments, the liquid phase is modeled as a regular solution, a model that cannot describe the chemical ordering observed in this system. For example, X-ray diffraction experiments reported by Lukens and Wagner[15] indicate the existence of chemical short range order in the liquid phase with Cu_2Mg and $CuMg_2$ stoichiometries. This discrepancy is clearly observed in the inability of these models to accurately describe the heat capacity of the undercooled liquid, as shown in Fig. 1. Second, these previous models treat the Mg_2Cu-C_b as a stoichiometric compound, precluding any description of nonequilibrium compositions for these phases. Finally, the models constrain the temperature dependence of the Gibbs free energy of this phase to be linear, implying that there is no contribution to the heat capacity from chemical mixing. Consequently, while the equilibrium phase diagram produced from these models may be useful, more fundamental thermodynamic quantities associated with these models, such as the heat capacity, do not agree well with experimental measurements, such as those reported by Feufel and Sommer.[16]

In the work presented here, we address each of these limitations within the framework of a general CAL-

Shihuai Zhou, Yi Wang, Long-Qing Chen, and **Zi-Kui Liu,** Department of Materials Science and Engineering, The Pennsylvania State University, University Park, PA 16802, USA; **Frank G. Shi,** Department of Chemical Engineering and Materials Science, University of California, Irvine, CA 92697, USA; **Ferdinand Sommer,** Max-Planck-Institute for Metals Research, Heisenbergstraße 3, D-70569 Stuttgart, Germany; **Shihuai Zhou** and **Ralph E. Napolitano,** Materials & Engineering Physics Program, Ames Laboratory, USDOE, Ames, IA, USA; **Ralph E. Napolitano,** Department of Materials Science and Engineering, Iowa State University, 116 Wilhelm Hall, Ames, IA, USA. Contact e-mail: ralphn@iastate.edu
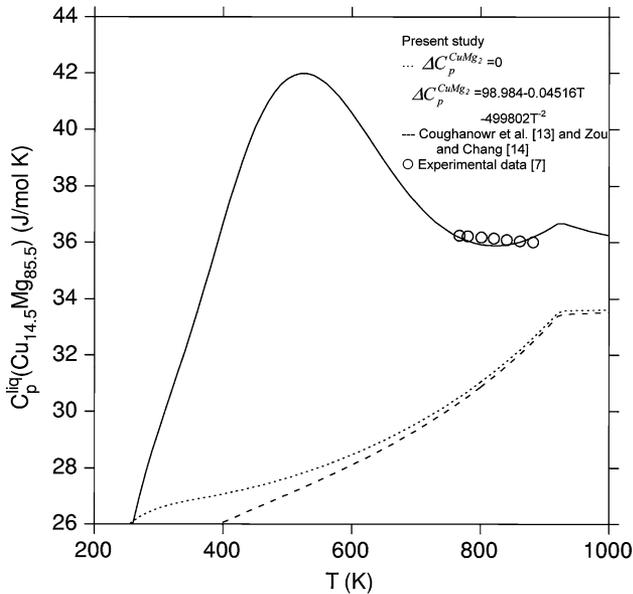
Fig. 1 The heat capacity of the liquid $Cu_{14.5}Mg_{85.5}$ alloy calculated using the parameters in Tables 2-4

PHAD[17,18] formulation by (i) employing an association model capable of describing the nonlinear temperature dependence of chemical short range order in the liquid phase and (ii) treating the intermetallic phases as substitutional solid solutions on two sublattices, permitting quantification of the Gibbs free energies of the intermetallic phases at non-stoichiometric compositions. In addition, we incorporate first-principles calculations to compute the zero-Kelvin energies of end-member phases in unstable structures, since experimental data are not available for these phases. Remaining model parameters, describing the Gibbs free energies associated with the formation of compounds or solution phases, are determined through a systematic semi-empirical optimization, employing available experimental data from calorimetry, X-ray diffraction, electron-probe microchemical analysis, and optical micrography.[7,16,19-40] The resulting thermodynamic properties and the associated equilibrium phase diagram are compared with the prior thermodynamic modeling reported by Coughanowr et al.[13] and by Zou and Chang.[14]

2. Thermodynamic Models

We describe the phase equilibria in the Cu-Mg binary system by modeling the Gibbs free energy for each relevant phase over the appropriate range of composition at constant pressure (1 atm). In any case where a temperature dependent parameter (P) is required, we use the general form,

$$P(T) = a + bT + cT \ln T + dT^2 + eT^{-1} + fT^3 + gT^7 + hT^{-9}$$
$$(Eq\ 1)$$

The thermodynamic properties of pure Cu and Mg in various structures are computed using the parameters from the SGTE database.[41] The liquid phase is described with an association model.[42,43] The terminal fcc and hcp solid solutions are treated with a single lattice while intermediate phases are described using a two-sublattice model,[44] where each sublattice is treated as a regular solution. In the following sections, the thermodynamic treatment of each phase is described in detail.

2.1 The Liquid Phase

We employ a four-species association model,[42,43] where Cu_2Mg and $CuMg_2$ are chosen as the relevant intermediate chemical associates.[15] Thus, the Gibbs free energy of the liquid phase is given by

$$G_m^{liq} = \sum_i x_i {}^\circ G_i^{liq} + RT \sum_i x_i \ln x_i + \sum_i \sum_{j>i} x_i x_j {}^\circ L_{i,j}^{liq},$$
$$(i,j = Cu, Cu_2Mg, CuMg_2, Mg) \qquad (Eq\ 2)$$

where x_i and ${}^\circ G_i^{liq}$ denote the mole fraction and molar Gibbs free energy for the ith species in the liquid phase, respectively, and where we have considered only pair-wise interaction between species. The Gibbs free energy of the intermediate associates, Cu_mMg_n, are given as

$${}^\circ G_{Cu_mMg_n}^{liq} = m {}^\circ G_{Cu}^{liq} + n {}^\circ G_{Mg}^{liq} + \Delta G_{Cu_mMg_n}^{liq}, \qquad (Eq\ 3)$$

where $\Delta G_{Cu_mMg_n}^{liq}$ represents the Gibbs free energy of formation. Substituting Eq 3 into Eq 2, the Gibbs free energy of the liquid phase is written as

$$\begin{aligned}
G_m^{liq} = &(x_{Cu} + 2x_{Cu_2Mg} + x_{CuMg_2}) {}^\circ G_{Cu}^{liq} \\
&+ (x_{Mg} + x_{Cu_2Mg} + 2x_{CuMg_2}) {}^\circ G_{Mg}^{liq} \\
&+ x_{Cu_2Mg} \Delta G_{Cu_2Mg}^{liq} + x_{CuMg_2} \Delta G_{CuMg_2}^{liq} \\
&+ RT(x_{Cu} \ln x_{Cu} + x_{Cu_2Mg} \ln x_{Cu_2Mg} + x_{CuMg_2} \ln x_{CuMg_2} \\
&+ x_{Mg} \ln x_{Mg}) + x_{Cu} x_{Cu_2Mg} {}^\circ L_{Cu,Cu_2Mg}^{liq} + x_{Cu} x_{CuMg_2} {}^\circ L_{Cu,CuMg_2}^{liq} \\
&+ x_{Cu} x_{Mg} {}^\circ L_{Cu,Mg}^{liq} + x_{CuMg_2} x_{Cu_2Mg} {}^\circ L_{CuMg_2,Cu_2Mg}^{liq} \\
&+ x_{Mg} x_{Cu_2Mg} {}^\circ L_{Cu_2Mg,Mg}^{liq} + x_{Mg} x_{CuMg_2} {}^\circ L_{CuMg_2,Mg}^{liq} \qquad (Eq\ 4)
\end{aligned}$$

The interaction energies $({}^\circ L_{i,j}^{liq})$ are described here as constants, while the Gibbs free energies of formation $(\Delta G_{Cu_mMg_n}^{liq})$ are described as functions of temperature, using the form given in Eq 1. Where sufficient heat capacity data are available, the parameters $a-e$ are used. Otherwise, we employ only parameters a and b. This will be discussed in further detail in a subsequent section.

2.2 Terminal fcc and hcp Phases

The fcc and hcp phases are treated as simple binary substitutional solutions with Gibbs free energies expressed as

$$G_m^\Phi = \sum_{i=Cu,Mg} x_i {}^\circ G_i^\Phi + RT \sum_{i=Cu,Mg} x_i \ln x_i + {}^{xs} G_m^\Phi \qquad (Eq\ 5)$$

where x_i denotes mole fraction of element i, and $°G_i^\Phi(i = \text{Cu, Mg})$ denotes the molar Gibbs free energy of the pure element i with the structure $\Phi(\Phi = \text{fcc or hcp})$. The excess Gibbs free energy $^{xs}G_m^\Phi$ is expressed as,

$$^{xs}G_m^\Phi = x_{\text{Cu}}x_{\text{Mg}}\sum_{j=0}^{n} {}^jL_{\text{Cu,Mg}}^\Phi(x_{\text{Cu}} - x_{\text{Mg}})^j \qquad \text{(Eq 6)}$$

where the $^jL_{\text{Cu,Mg}}^\Phi$ coefficients are left as interaction parameters to be evaluated with experimental data. Here, we consider only the $j = 0$ term and assume that $°L_{\text{Cu,Mg}}^\Phi$ is constant (i.e., a regular solution).

2.3 Intermediate Cu₂Mg-C15 and Mg₂Cu-C_b Phases

Using a two-sublattice model, we describe each intermediate compound as a solid solution of the form $(\text{Cu,Mg})_2(\text{Cu,Mg})_1$. The Gibbs free energy is given as

$$G_m^\theta = \sum_{i=\text{Cu,Mg}} y_i^I \sum_{j=\text{Cu,Mg}} y_j^{II}°G_{i:j}^\theta + RT$$
$$\sum_{i=\text{Cu,Mg}} (2y_i^I \ln y_i^I + y_i^{II} \ln y_i^{II}) + {}^{xs}G_m^\theta \qquad \text{(Eq 7)}$$

where the colon separates the components on different sublattices, and y^I and y^{II} are the sublattice site occupancy fractions. The superscript, θ, represents the Cu₂Mg-C15 or Mg₂Cu-C_b structure.

With the sublattice description we have adopted, each of the two structures (C15 and C_b) can assume four different stoichiometries (Cu₂Cu, Mg₂Cu, Cu₂Mg, and Mg₂Mg), with only one being that of the stable compound. These are Cu₂Mg-C15 and Mg₂Cu-C_b, and, for these compounds, we express $°G_{\text{Cu:Mg}}^{\text{C15}}$ and $°G_{\text{Mg:Cu}}^{\text{C}_b}$ using the form given in Eq 1 and evaluate the related coefficients using available enthalpy of formation, melting temperature, and heat capacity data, as discussed in a subsequent section. For the unstable compounds (i.e., Cu₂Cu-C15, Mg₂Cu-C15, Mg₂Mg-C15, Cu₂Cu-C_b, Cu₂Mg-C_b, and Mg₂Mg-C_b), there are no available heat capacity data with which to evaluate the coefficients c-g. Therefore, we express the Gibbs free energy as

$$°G_{i:j}^\theta = 2\,°G_i^{\text{ref}} + °G_j^{\text{ref}} + \Delta G_{i:j}^\theta, \quad (i,j = \text{Cu, Mg}) \qquad \text{(Eq 8)}$$

where $°G_i^{\text{ref}}$ and $°G_j^{\text{ref}}$ are the molar Gibbs free energy of either fcc-Cu or hcp-Mg, and $\Delta G_{i:j}^\theta$ is the Gibbs free energy of formation for the compound $(i)_2(j)_1$ from the $2(i) + (j)$ mixture, which we treat as a constant. The excess Gibbs free energy term in Eq 7 is modeled as,

$$^{xs}G_m^\theta = y_{\text{Cu}}^I y_{\text{Mg}}^I \sum_{i=\text{Cu,Mg}} y_i^{II} \sum_{k=0} {}^kL_{\text{Cu,Mg}:i}^\theta(y_{\text{Cu}}^I - y_{\text{Mg}}^I)^k$$
$$+ y_{\text{Cu}}^{II} y_{\text{Mg}}^{II} \sum_{i=\text{Cu,Mg}} y_i^I \sum_{k=0} {}^kL_{i:\text{Cu,Mg}}^\theta(y_{\text{Cu}}^{II} - y_{\text{Mg}}^{II})^k \qquad \text{(Eq 9)}$$

Once again, we consider only the $k = 0$ term in each inner sum, and assume that $°L^\theta$ is a constant.

2.4 Calculation of Zero-Kelvin Enthalpies from First Principles

To facilitate the determination of the Gibbs free energy of formation for the intermediate compound phases, we compute the enthalpy of formation for the end-members at zero Kelvin. For these calculations, we employ the VASP[45] implementation of the plane wave method using the Vanderbilt ultrasoft pseudopotential[46] with a generalized gradient approximation (GGA).[47] The Monkhost 15×15×15 k points are employed for high precision calculations. The $3s3p$ and $3d4s4p$ shells are treated as valence states with core radii of 2.88 a.u. and 2.48 a.u. for the hcp-Mg and fcc-Cu, respectively. To ensure that the unit cell corresponds to a stable structure, we fully relax the cell shape and the internal atomic coordinates of the stable end-members of the compounds and relax only the cell volumes of those end-members which are unstable.

The enthalpy of formation, ΔH_f^ϕ, of a compound φ is calculated as the difference between the energy of the compound and the linear combination of the energies of the pure elements in their reference states,

$$\Delta H_f^\phi = E^\phi - x_{\text{Cu}}^\phi E_{\text{Cu}}^{\text{fcc}} - x_{\text{Mg}}^\phi E_{\text{Mg}}^{\text{hcp}}, \qquad \text{(Eq 10)}$$

where x_i^ϕ is the mole fraction of component i in the ϕ structure. The values of $E^\phi, E_{\text{Cu}}^{\text{fcc}}$, and $E_{\text{Mg}}^{\text{hcp}}$ are the computed zero-Kelvin energies of the indicated phases, each considered here to be stoichiometric. The calculated results are listed in Table 1 and compared with experimental data. Again, we note here that for the stable phases (Cu₂Mg-C15 and Mg₂Cu-C_b), both experimental and first-principles data are considered in our evaluation of thermodynamic parameters. For the unstable intermetallic phases ($\Delta H_f > 0$), however, experimental data are not attainable and the zero-Kelvin energies become essential in assessing the relative stability of these compounds. The determination of model parameters is discussed in the next section.

3. Determination of the Thermodynamic Model Parameters

Expressions for the standard Gibbs free energy ($°G_i^\phi$) of each pure component in the relevant phases are taken from the SGTE database[41] as listed in Table 2. In addition, based on the models described in the preceding sections, we compute a standard Gibbs free energy for each of the two intermediate compounds and evaluate the parameters, as listed in Table 3. For the relevant excess Gibbs free energies, we employ a total of eight Gibbs free energy of formation terms and 12 interaction parameters (four of which we assume to be equal to zero). These are listed in Table 4, along with the results from our parameter evaluation. In the present section, the methodology used for determination of the parameters listed in Tables 3 and 4 is discussed.

Table 1   A summary of the results from the first-principles calculations

| | | ΔH, kJ/mol of atoms | | |
| | | First principles | Modeling | Experiment |
Phase	Formula	0 K	298 K	
Cu-fcc	Cu	0	…	…
Mg-hcp	Mg	0	…	…
Cu_2Mg-C_{15}	Cu_2Cu	15.5	15.5	…
	Cu_2Mg	−15.72	−11.4	−11.3[36] −8.04[37]
	$CuMg_2$	34.72	34.72	…
	Mg_2Mg	7.00	7.00	…
$CuMg_2$-C_b	Cu_2Cu	20.39	20.39	…
	Cu_2Mg	38.94	38.94	…
	$CuMg_2$	−13.20	−9.6	−9.55[36]
	Mg_2Mg	12.92	12.92	…

Table 2   The thermodynamic parameters for pure Cu and Mg[41]

Cu phases	$^\circ G_{Cu}^{liq}$		$^\circ G_{Cu}^{fcc}$		$^\circ G_{Cu}^{hcp}$
T_{min}, K	298	1357.77	298	1357.77	298
T_{max}, K	1357.77	3200	1357.77	3200	3200
$^\circ G^{ref}$	$^\circ G_{Cu}^{fcc}$	0	0	0	$^\circ G_{Cu}^{fcc}$
a	12964.735	−46.545	−7770.458	−13542.026	600
b	−9.511904	173.881484	130.485235	183.803828	0.2
c	…	−31.38	−24.112392	− 31.38	…
d	…	…	$−2.65684\times10^{-3}$	…	…
e	…	…	52478	…	…
f	…	…	1.29223×10^{-7}	…	…
g	$−5.8489\times10^{-21}$	…	…	…	…
h	…	…	…	3.64167×10^{29}	…

Mg phases	$^\circ G_{Mg}^{liq}$		$^\circ G_{Mg}^{fcc}$		$^\circ G_{Mg}^{hcp}$
T_{min}	298	923	298	298	923
T_{max}	923	3000	3000	923	3000
$^\circ G^{ref}$	$^\circ G_{Mg}^{hcp}$	0	$^\circ G_{Mg}^{hcp}$	0	0
a	8202.243	−5439.869	2600	−8367.34	−14130.185
b	−8.83693	195.324057	−0.9	143.675547	204.716215
c	…	−34.3088	…	−26.1849782	−34.3088
d	…	…	…	4.858×10^{-4}	…
e	…	…	…	78950	…
f	…	…	…	$−1.393669\times10^{-6}$	…
g	$−8.0176\times10^{-20}$	…	…	…	…
h	…	…	…	…	1.038192×10^{28}

Note: $^\circ G_i^\theta = {}^\circ G^{ref} + a + bT + cT\,ln\,T + dT^2 + eT^{-1} + fT^3 + gT^7 + hT^{-9}$ (J/mol)

For the liquid phase, we evaluate the parameters $\Delta G_{Cu_mMg_n}^{liq}$ and $^\circ L_{i,j}^{liq}$, from Eq 2-3, using reported values of activity,[33] chemical potential,[30-35] and enthalpy of mixing.[29,30] Initially we model $\Delta G_{Cu_mMg_n}^{liq}$ using only the first two terms in Eq 1 (i.e., $a + bT$). This treatment, shown in Fig. 1, yields a heat capacity for $Cu_{15.5}Mg_{84.5}$ liquid that is slightly higher than the models of Coughanowr et al.[13] and Zou and Chang,[14] but one that remains much lower than the reported experimental data.[7] We assert that this apparent excess heat capacity may be due to chemical (and perhaps structural) ordering in the liquid phase over this range of temperatures. Accordingly, we describe the associated nonlinear temperature dependence by fitting the parameters c-e in Eq 1 for $\Delta G_{CuMg_2}^{liq}$. The evaluated results are listed in Table 4 and the corresponding heat capacity is also plotted in Fig. 1, where a maximum in the $C_p(T)$ curve is exhibited. We note that such maxima in $C_p^{liq}(T)$ have been observed in a number of systems (e.g., toluene, Au-Si,

Table 3 Ground state standard Gibbs free energy parameters for the intermetallic phases Cu_2Mg-C15 and Mg_2Cu-C_b

$^\circ G_{i:j}^0$	$^\circ G_{Cu:Mg}^{C15}$, J/mol		$^\circ G_{Mg:Cu}^{C_b}$, J/mol	
T_{min}, K	298	1070	298	850
T_{max}, K	1070	…	850	…
$^\circ G^{ref}$	0	0	0	0
a	−58201	−64662.18	−53491	−58610.6334
b	409.642	490.7029614	425.428	481.9243846
c	−76.1	−87.17102875	−77.9913484	−85.33353573
d	-9.9×10^{-4}	…	2.31×10^{-3}	…
e	183906	…	190378	…
f	-1.35×10^{-6}	…	-2.72115×10^{-6}	…
g	…	…	…	…
h	…	…	…	…

Table 4 Excess Gibbs free energy parameters (all temperatures)

Phase	Parameters	Value, J/mol
Liquid	$\Delta G_{Cu_2Mg}^{liq}$	$-28312 + 9.595\,T$
	$\Delta G_{CuMg_2}^{liq}$	$-108077 + 748.301\,T - 98.984$ $T \ln(T) + 0.02258\,T^2 + 2499901\,T^{-1}$
	$^\circ L_{Cu,Cu_2Mg}^{liq}$	−20012
	$^\circ L_{Cu,CuMg_2}^{liq}$	−24230
	$^\circ L_{Cu,Mg}^{liq}$	−22611
	$^\circ L_{Cu_2Mg,CuMg_2}^{liq}$	0
	$^\circ L_{Cu_2Mg,Mg}^{liq}$	−25845
	$^\circ L_{CuMg_2,Mg}^{liq}$	0
hcp	$^\circ L_{Cu,Mg:Va}^{hcp}$	39230
fcc	$^\circ L_{Cu,Mg:Va}^{fcc}$	−19345
$CuMg_2$-C15	$\Delta G_{Cu:Cu}^{C15}$	46500
	$\Delta G_{Mg:Cu}^{C15}$	104160
	$\Delta G_{Mg:Mg}^{C15}$	21000
	$^\circ L_{Cu:Cu,Mg}^{C15}$	−27868
	$^\circ L_{Cu,Mg:Mg}^{C15}$	3521
$CuMg_2$-C_b	$\Delta G_{Cu:Cu}^{C_b}$	61170
	$\Delta G_{Cu:Mg}^{C_b}$	116820
	$\Delta G_{Mg:Mg}^{C_b}$	38760
	$^\circ L_{Cu:Cu,Mg}^{C_b}$	0
	$^\circ L_{Cu,Mg:Mg}^{C_b}$	0

As_2Se_3,[48] $La_{20}Mg_{50}Ni_{30}$, $Al_{30}La_{50}Ni_{20}$, $Al_{7.5}Cu_{17.5}$-$Ni_{10}Zr_{65}$,[49] $Al_{7.5}Cu_{27.5}Zr_{65}$,[50]) again suggesting some type of clustering/ordering reaction in the liquid phase.

The interaction parameter for each of the terminal solid solution phases is determined from experimental estimates of the respective solidus and solvus boundaries, where the solubility of Cu in the hcp-Mg phase has been reported to be 0.15, 0.23, and 0.23 at.% by Hansen,[25] Stepanov and Kornilov,[26] and Yue and Pierre,[27] respectively. The resulting interaction parameter for the hcp solution phase is high and positive, as listed in Table 4. For the fcc solid solution, the interaction parameter listed in Table 4 is determined from the fcc phase boundary data reported by Jones[22] and Rogelberg.[23]

Regarding the intermediate compounds and the evaluation of coefficients in the expressions for $^\circ G_{Cu:Mg}^{C15}$ and $^\circ G_{Mg:Cu}^{C_b}$, as in Eq 1 and 7, we require experimental or theoretical values for heat capacity, enthalpy of formation, and melting temperature. The parameters that contribute to the heat capacity (i.e., coefficients c-f in Eq 1 are evaluated using the experimental results of Feufel and Sommer,[16] recognizing that, above their melting temperatures, the heat capacities of the Cu_2Mg-C15 and Mg_2Cu-C_b phases should approach that of the liquid phase, as given by the SGTE model.[41] The available enthalpy of formation data include only the stable Cu_2Mg-C15 and Mg_2Cu-C_b phases. They are listed in Table 1 along with our first principles calculations, which include these phases as well as the unstable compounds for which experimental data are not available. In addition, we consider the electromotive force (EMF) measurements of activity and chemical potential, reported by Arita et al.[38] and Eremenko et al.[39] for the Cu-Mg binary system. These are shown in Fig. 2 and compared with the values of chemical potential associated with our first principles calculations and with experimental measurements of ΔH_f.[36,37] In this figure, the fcc/Cu_2Mg-C15 coexistence curve suggests that the experimental values reported by King and Kleppa[36] may be the most accurate, since they exhibit excellent agreement with the EMF data of Eremenko et al.[39] Based on this selection and the heat capacity considerations discussed above, the coefficients listed in Table 3 for $^\circ G_{Cu:Mg}^{C15}$ and $^\circ G_{Mg:Cu}^{C_b}$ are evaluated with the corresponding experimental data.[16,21,22,24,36,38,39] Finally, the two interaction parameters for the Cu_2Mg-C15 phase $(^\circ L_{Cu:Cu,Mg}^{C15}$ and $^\circ L_{Cu,Mg:Mg}^{C15})$ are evaluated using available phase equilibrium data.[20-24] The Gibbs free
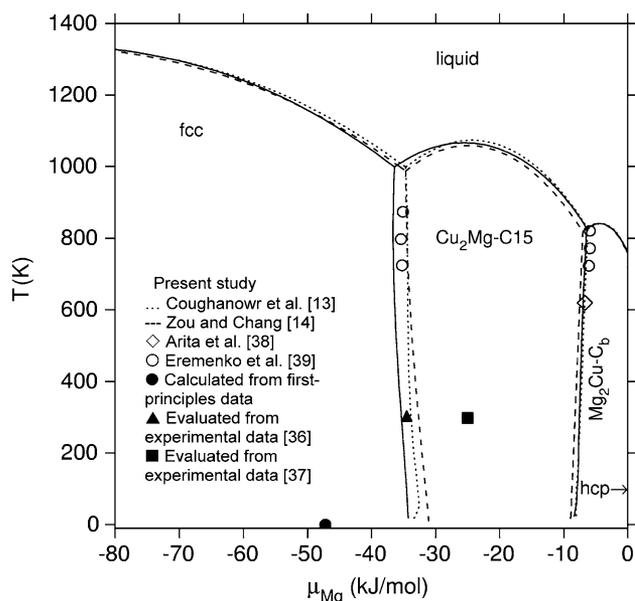

Fig. 2 The chemical potential of Mg associated with the indicated two-phase equilibrium, plotted over the relevant temperature range for the Cu-Mg system. The solid curves are computed and compared with prior modeling and experiment. The reference states are fcc-Cu and hcp-Mg

energy of formation, $\Delta G_{i:j}^{\theta}$, for each unstable end-member in Eq 8, is treated as a constant and determined using the first-principles data in Table 1. The parameter assessment

practice is iterative and culminates with an optimized fit involving all selected data and calculation results. The final parameters from the overall optimization are listed in Tables 3 and 4.
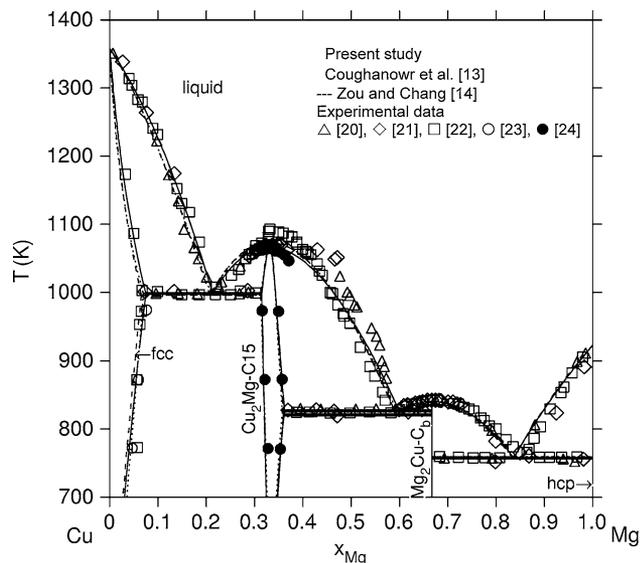
4. Phase Equilibrium Results

The phase diagram yielded by our modeling effort is shown in Fig. 3 along with previously proposed phase diagrams and relevant experimental data. In Table 5, the invariant reactions are compared with experimental reports[20-22] and with the models of Coughanowr[13] and Zou and Chang.[14] We note that the equilibrium phase boundaries produced by our model do not differ significantly from prior reports, except that our results may exhibit slightly better agreement with experimental liquidus and solidus data for the terminal solution phases. However, there are several important features of our thermodynamic description of this binary system that do differ substantially from previously reported models but are not dramatically evident in the equilibrium phase diagram itself. These differences primarily arise from (i) the use of chemical associates in our treatment of the liquid, (ii) our two-sublattice solution description of the intermediate phases, and (iii) inclusion of non-linear temperature dependent free energies of formation, all of which offer improvements over prior treatments

Fig. 3 The Cu-Mg phase diagram calculated using the parameters listed in Tables 2-4, shown with the relevant experimental data

Table 5 Invariant reactions in the Cu-Mg system

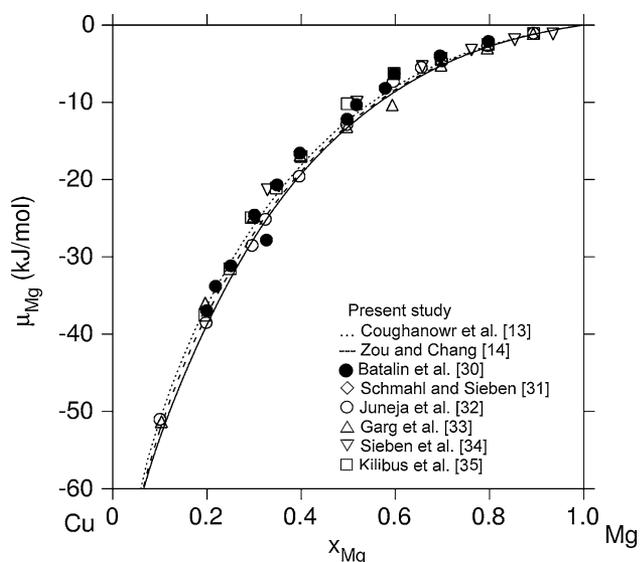| Reaction		Calculated results			Experimental data
		This work	Ref.[13]	Ref.[14]	
Liq → Cu₂Mg-C15	T, K	1066.3	1073.0	1066.2	1063[20]
					1070[21]
					1092[22]
					1066[24]
	$x_{(liquid,\ Mg)}$	0.333	0.333	0.333	0.333[24]
	$x_{(C15,\ Mg)}$	0.333	0.333	0.333	0.333[24]
Liq → CuMg₂-C$_b$	T, K	840.5	841	841	841[22,24]
	$x_{(liquid,\ Mg)}$	0.667	0.667	0.667	0.667[24]
	$x_{(Cb,\ Mg)}$	0.667	0.667	0.667	0.667[24]
Liq → fcc + Cu₂Mg-C15	T, K	998.8	998	998.3	995[22]
					998[20,24]
	$x_{(liquid,\ Mg)}$	0.213	0.209	0.214	0.230[20]
	$x_{(fcc,Mg)}$	0.074	0.069	0.075	0.069[24]
	$x_{(C15,Mg)}$	0.314	0.313	0.316	0.310[24]
Liq → CuMg₂-C$_b$ + Cu₂Mg-C15	T, K	826.5	825.5	825.2	828[20,21]
					825[22,24]
	$x_{(liquid,\ Mg)}$	0.594	0.595	0.588	0.585[20]
	$x_{(Cb,Mg)}$	0.667	0.667	0.667	0.667[20]
	$x_{(C15,Mg)}$	0.361	0.356	0.359	0.353[20]
Liq → hcp + CuMg₂-C$_b$	T, K	757.3	759.0	758.0	753[20]
					758[21,22]
	$x_{(liquid,\ Mg)}$	0.838	0.839	0.841	0.855[21,22]
	$x_{(hcp,Mg)}$	1.000	1.000	1.000	1[22]
	$x_{(Cb,Mg)}$	0.667	0.667	0.667	0.667[22]

Fig. 4 The chemical potential of Mg as a function of composition for the Cu-Mg liquid phase calculated for 1,100 K and compared with prior modeling and experiment. The reference states are liq-Cu and liq-Mg
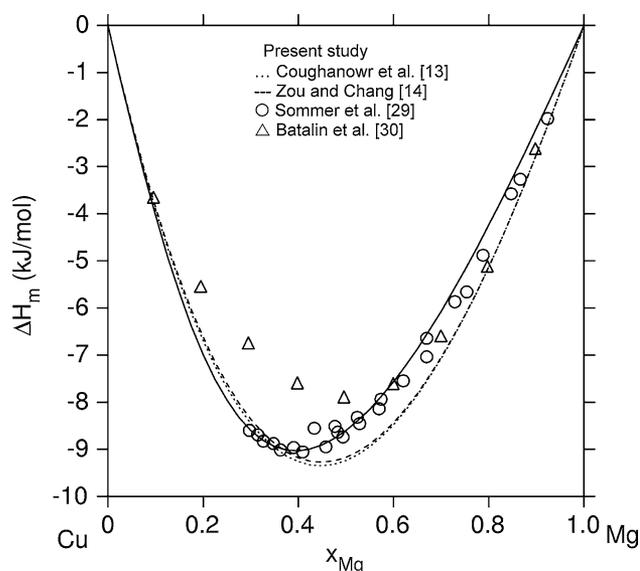

Fig. 6 The enthalpy of mixing of the liquid phase calculated for 1,120 K and compared with prior modeling and experiment. The reference states are liq-Cu and liq-Mg
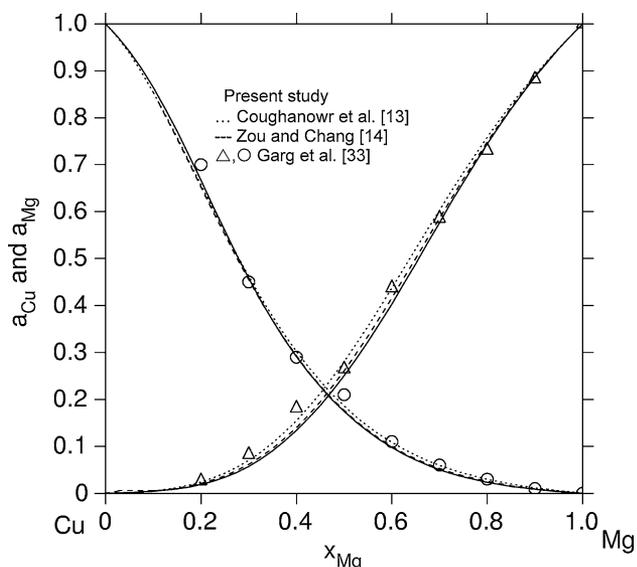

Fig. 5 The activity of Cu and Mg calculated for 1,200 K and compared with prior modeling and experiment. The reference states are liq-Cu and liq-Mg

Table 6 The melting enthalpies of the compounds Cu_2Mg-C15 and Mg_2Cu-C_b

	Calculated results, kJ/mol			Experimental data, kJ/mol[16]
Compound	This work	Ref.[13]	Ref.[14]	
Cu_2Mg-C15	14.1	12.4	13.5	15.2 ± 1.5
Mg_2Cu-C_b	12.3	11.5	11.4	13.7 ± 1.5

and permit the quantitative description of thermodynamic parameters for both undercooled liquids and nonequilibrium compositions of the intermetallic phases.

Figures 4 and 5 show that there is little difference between prior models and ours with regard to quantification of chemical potential of the liquid phase over the full range of composition at 1100 K and 1200 K. However, Fig. 6 shows that our model provides much better agreement with

the experimental measurements of enthalpy of mixing for the liquid phase, as reported by Sommer et al.[29] This feature is essential if driving forces for various phase transitions involving both equilibrium and nonequilibrium compositions of the relevant phases are to be computed accurately and compared. In addition, we employ the temperature-dependent description given in Eq 1 for the Gibbs free energy of Cu_2Mg-C15 and Mg_2Cu-C_b rather than the simpler description used in earlier reports.[13,14] As a result, it is clear from Fig. 7 that our description reproduces the experimental heat capacity data[16] far better than previously reported models.[13,14] In addition, the modeled melting enthalpies for Cu_2Mg-C15 and Mg_2Cu-C_b are listed in Table 6, where our results show better agreement with the experimental data for these phases[16] than those reported by Coughanowr et al.[13] and Zou and Chang.[14] Finally, for the purpose of further direct comparison, we include in Fig. 1 our modeling results for the heat capacity of the $Cu_{14.5}Mg_{85.5}$ liquid, showing the dramatic improvement in low-temperature heat capacity compared to the models by Coughanowr et al.[13] and Zou and Chang.[14]
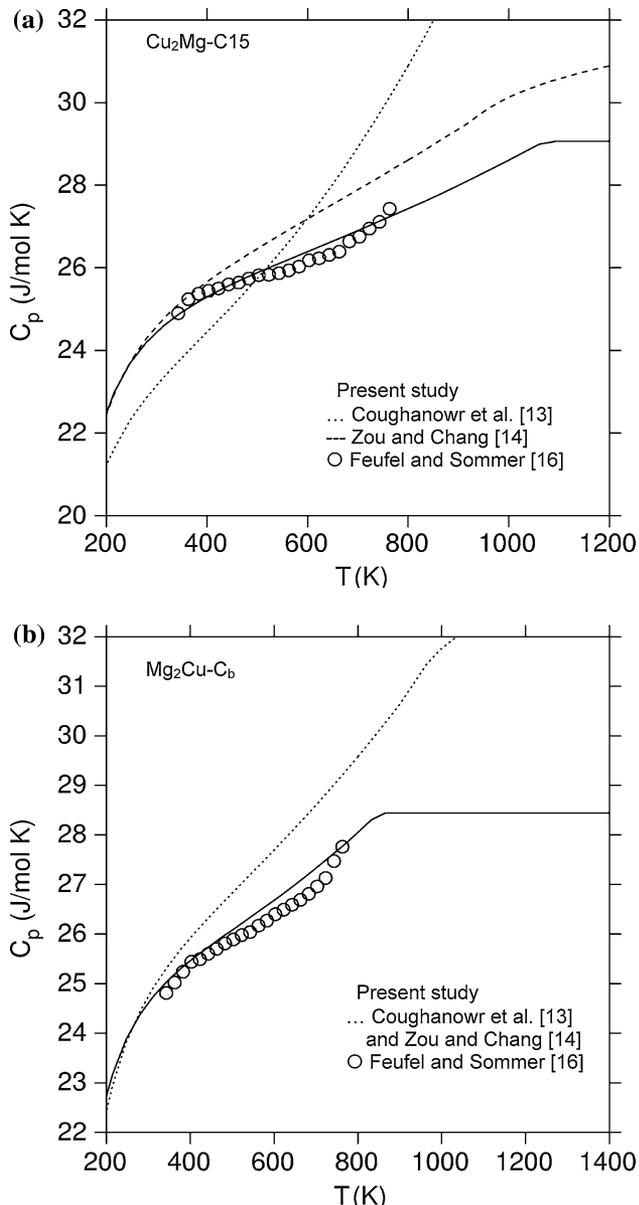
Fig. 7 The heat capacity (a) Cu_2Mg-C15 and (b) Mg_2Cu-C_b computed using our model parameters in Tables 1-3 and compared with previously reported models and data

5. Summary and Conclusions

Employing a solution thermodynamics approach, the Gibbs free energy vs. composition curves for all relevant phases in the Cu-Mg binary system were estimated, and the associated binary phase diagram is reported here. While the resulting equilibrium phase diagram exhibits only modest deviation from previously reported diagrams, the current thermodynamic description exhibits several key differences from earlier thermodynamic models. These differences arise from (i) the two-sublattice solution treatment of the Mg_2Cu-

C_b phase, (ii) the use of first principles calculations to obtain the zero-Kelvin energies for the unstable compounds, and (iii) the use of an association model for the liquid phase. As a result, the current model provides a more realistic quantification of heat capacity for the relevant phases and a better description of the composition-dependent enthalpy of mixing for the liquid.

Acknowledgments

References

1. A. Inoue and A. Takeuchi, Recent Progress in Bulk Glassy Alloys, *Mater. Trans., JIM,*, 2002, **43**, p 1892-1906
2. A. Inoue, H. Kimura, and A. Takeuchi, in *Thermec-2003*, TRANS TECH PUBLICATIONS LTD, Zurich-Uetikon, 2003, vol. 426-4, p 3-10
3. J.F. Loffler, Bulk Metallic Glasses, *Intermetallics*, 2003, **11**, p 529-540
4. A. Inoue and A. Takeuchi, Recent Progress in Bulk Glassy, Nanoquasicrystalline and Nanocrystalline Alloys, *Mater. Sci. Eng., A*, 2004, **375-377**, p 16-30
5. S.H. Zhou and R.E. Napolitano, Phase Equilibria and Thermodynamic Limits for Partitionless Crystallization in the Al-La Binary System, *Acta Mater.*, 2006, **54**, p 831-840
6. A. Inoue, Amorphous, Nanoquasicrystalline and Nanocrystalline Alloys in Albased Systems, *Prog. Mater. Sci.*, 1998, **43**, p 365-520
7. F. Sommer, G. Bucher, and B. Predel, Thermodynamic Investigations of Mg-Cu and Mg-Ni Metallic Glasses, *J. Phys. Colloq.*, 1980, **C8**, p 563-566
8. T. Masumoto and R. Maddin, Structural Stability and Mechanical Properties of Amorphous Metals, *Mater. Sci. Eng.*, 1975, **19**, p 1-24
9. T. Masumoto and R. Maddin, Mechanical Properties of Pd-20 At. Percent Si Alloy Quenched from the Liquid State, *Acta Met.*, 1971, **19**, p 725-741
10. W.L. Johnson, In: H. Beck, H.J. Guntherodt, Eds., *Glassy Metals*, Springer-Verlag, Berlin, 1983
11. F.P. Messel, S. Frota-Pessoa, J. Wood, J. Tyler, and J.E. Keem, Electronic Density of States in Amorphous Zirconium Alloys, *Phys. Rev. B*, 1983, **27**, p 1596-1604
12. M. Tenhover and W.L. Johnson, Superconductivity and the Electronic Structure of Zr- and Hf-based Metallic Glasses, *Phys. Rev. B*, 1983, **27**, p 1610-1618
13. C.A. Coughanowr, I. Ansara, R. Luoma, M. Hamalainen, and H.L. Lukas, Assessment of the Cu-Mg System, *Z. Metallkd.*, 1991, **82**, p 574-581
14. Y. Zou and Y.A. Chang, Thermodynamic Calculation of the Mg-Cu Phase Diagram, *Z. Metallkd.*, 1993, **84**, p 662-667
15. W.E. Lukens and C.N.J. Wagner, The Structure of Liquid Cu-Mg Alloys, *Z. Naturforsch.*, 1973, **28**, p 297-304
16. H. Feufel and F. Sommer, Thermodynamic Investigations of Binary-Liquid and Solid Cu-Mg and Mg-Ni Alloys and Ternary Liquid Cu-Mg-Ni Alloys, *J. Alloy. Compd.*, 1995, **224**, p 42-54
17. L. Kaufman and H. Bernstein, *Computer Calculation of Phase Diagrams*. Vol. 4, Academic Press Inc., New York, 1970

18. N. Saunders and A.P. Miodownik, *CALPHAD (Calculation of Phase Diagrams): A Comprehensive Guide*, Pergamon, Oxford, New York, 1998

19. G. Grime and W. Morris-Jones, An X-ray Investigation of the Copper-Magnesium Alloys, *Phil. Mag.*, 1929, **7**, p 1113-1134

20. G.G. Urazova, Experimental Measurements for Cu-Mg System, *Zh. Russ. Fiz-Khim. Obschestva*, 1907, **39**, p 1556-1581

21. R. Sahmen, Metallographic Announcements from the Institute for Inorganic Chemistry of the University of Gottingen LVIII Concerning the Alloys of Copper with Cobalt, Iron, Manganese and Magnesium, *Z. Anorg. Chem.*, 1908, **57**, p 1-33

22. W.R.D. Jones, The copper-magnesium Alloys. Part IV. The Equilibrium Diagram, *J. Inst. Met.*, 1931, **46**, p 395-419

23. I.L. Rogelberg, Cu-Mg Phase Diagram, *Tr. Gos. Nauchn. -Issled.*, 1957, **16**, p 82-89

24. P. Bagnoud and P. Feschotte, Binary Systems Mg-Cu and Mg-Ni, Particularly the Non-Stoichiometry of the MgCu2 and MgNi2 Laves Phases, *Z. Metallkd.*, 1978, **69**, p 114-120

25. M. Hansen, Note on the Magnesium-Rich Magnesium-Copper Alloys, *J. Inst. Met.*, 1927, **37**, p 93-100

26. N.I. Stepanov and I.I. Kornilov, Solubility of copper in magnesium in the solid state, *Izvestiya Instituta Fiziko-Khimicheskogo Analiza*, 1935, **7**, p 89-98

27. A.S. Yue and R.S. Pierre, Ed., *Metall. Soc. Conf., New York*, Interscience Publishers, Inc., 1961, p 613-615

28. J.W. Jenkin, *J. Inst. Met.*, 1927, **37**, p 100-101

29. F. Sommer, J.J. Lee, and B. Predel, Calorimetric Investigations of Liquid Alkaline Earth Metal Alloys, *Ber. Bunsenges. Phys. Chem.*, 1983, **87**, p 792-797

30. G.I. Batalin, V.S. Sudavtsova, and M.V. Mikhailovskaya, Thermodynamic Properties of Liquid Alloys of the Cu–Mg Systems, *Izv. V.U.Z. Tsvetn. Metall.*, 1987, **2**, p 29-31

31. N.G. Schmahl and P. Sieben, *NPL Symposium 9 on Phys. Chem. of Metallic Solutions and Intermetallic Compounds, London*, HMSO, 1958, p 1-16

32. J.M. Juneja, G.N.K. Iyengar, and K.P. Abraham, Thermodynamic Properties of Liquid (Magnesium + Copper) Alloys By Vapor-Pressure Measurements Made By a Boiling-Temperature Method, *J. Chem. Thermodyn.*, 1986, **18**, p 1025-1035

33. S.P. Garg, Y.J. Bhatt, and C.V. Sundaram, Thermodynamic Study of Liquid Cu-Mg Alloys by Vapour Pressure Measurements, *Metall. Trans.*, 1973, **4**, p 283-289

34. P. Sieben and N.G. Schmahl, *Giesserei*, 1966, **18**, p 197-201

35. A.V. Kilibus, A.A. Gorshkov, and B.M. Lepinskii, *Trans. Inst. Met. Severdlosk.*, 1969, **18**, p 55-62

36. R.C. King and O.J. Kleppa, A thermochemical Study of Some Selected Laves Phases, *Acta Metall.*, 1964, **12**, p 87-97

37. B. Predel and H. Ruge, Beitrag zur Frage nach den Bindungsverhaltnissen in Laves-Phsen, *Mater. Sci. Eng.*, 1972, **9**, p 333-339, (in German)

38. M. Arita, Y. Ichinose, and M. Someno, *Thermodynamic Properties of the Ti-Cu, Ti-Ni and Mg-Cu Systems by Metal-Hydrogen Equilibration*, Metall. Soc. AIME, Warrendale, PA, 1981, p 153-158

39. V.N. Eremenko, G.M. Lukashenko, and R.I. Polotskaya, Thermodynamic Properties of Magnesium-Copper Compounds, *Russ. Met.*, 1968, **1**, p 126-129

40. A.T.W. Kempen, H. Nitsche, F. Sommer, and E.J. Mittemeijer, Crystallization Kinetics of Amorphous Magnesium-Rich Magnesium-Copper and Magnesium-Nickel Alloys, *Metall. Mater. Trans. A*, 2002, **33**, p 1041-1050

41. A.T. Dinsdale, SGTE Data for Pure Elements, *CALPHAD*, 1991, **15**, p 317-425

42. F. Sommer, Association Model for the Description of the Thermodynamic Functions of Liquid Alloys—Basic Concepts, *Z. Metallkd.*, 1982, **73**, p 72-86

43. H.G. Krull, R.N. Singh, and F. Sommer, Generalised Association Model, *Z. Metallkd.*, 2000, **91**, p 356-365

44. B. Sundman and J. Agren, A Regular Solution Model for Phases with Several Components and Sublattices, Suitable for Computer Applications, *J. Phy. Chem Solids*, 1981, **42**, p 297-301

45. G. Kresse, T. Demuth, and F. Mittendorfer, VAMP/VASP, http://www.cms.mpi.univie.ac.at/vasp/, 2003

46. D. Vanderbilt, Soft Self-Consistent Pseudopotentials in a Generalized Eigenvalue Formalism, *Phys. Rev. B*, 1990, **41**, p 7892-7895

47. G. Kresse and D. Joubert, From Ultrasoft Pseudopotentials to the Projector Augmented-wave Method, *Phys. Rev. B*, 1999, **59**, p 1758-1775

48. C.A. Angell, Formation of Glasses from Liquids and Biopolymers, *Science*, 1995, **267**, p 1924-1935

49. F. Sommer, Thermodynamics of Liquid Alloys, *Mater. Sci. Eng. A*, 1997, **226**, p 757-762

50. S.H. Zhou, J. Schmid, and F. Sommer, Thermodynamic Properties of Liquid, Undercooled Liquid and Amorphous Al-Cu-Zr and Al-Cu-Ni-Zr Alloys, *Thermochim. Acta*, 1999, **339**, p 1-9